Hindawi Publishing Corporation
International Journal of Photoenergy
Volume 2011, Article ID 305650, 14 pages
doi:10.1155/2011/305650

Research Article

Effect of Preparation Condition of TiO_2 Film and Experimental Condition on CO_2 Reduction Performance of TiO_2 Photocatalyst Membrane Reactor

Akira Nishimura,[1] Yuki Okano,[1] Masafumi Hirota,[1] and Eric Hu[2]

[1] *Division of Mechanical Engineering, Graduate School of Engineering, Mie University, 1577 Kurimamachiya-cho, Tsu 514-8507, Japan*
[2] *School of Mechanical Engineering, The University of Adelaide, Adelaide, SA 5005, Australia*

Correspondence should be addressed to Akira Nishimura, nisimura@mach.mie-u.ac.jp

Received 3 May 2011; Revised 29 June 2011; Accepted 19 July 2011

Academic Editor: Nicolas Alonso-Vante

It was previously reported that CO_2 could be reduced into CO, CH_4, and so forth, which can be used as fuels, by TiO_2 as the photocatalyst under UV radiation. To increase the concentration of fuel and improve CO_2 reduction performance on TiO_2 photocatalyst, a membrane reactor composed of TiO_2 and gas separation membrane prepared by sol-gel and dip-coating method has been built. Factors such as rising speed (RS) in the dip-coating process and the timing and amount of water injected in the membrane reactor in CO_2 reduction experiment have been investigated. As a result, the largest amount of TiO_2 film is obtained for RS = 0.66 mm/s among various RS conditions investigated in this study. According to CO_2 reduction experiment by gas circulation type reactor, too much water which cannot be consumed in CO_2 reduction process would not help improving the CO_2 reduction performance.

1. Introduction

It is reported that CO_2 can be reduced into fuels, for example, CO, CH_4, CH_3OH, H_2, and so forth, by using TiO_2 as the photocatalyst under ultraviolet (UV) light illumination [1–10]. If this technique could be applied practically, a carbon circulation system would then be established: CO_2 from the combustion of fuel is reproduced, using solar energy, to fuels again, and true zero emission can be achieved. Many R&D works on this technology have been carried out, using TiO_2 particles loaded with Cu, Pd, and Pt to react with CO_2 dissolved in solution [1, 5, 7, 11–17]. Recently, nanoscaled TiO_2 [18–20], porous TiO_2 [21], TiO_2 film combined with metal [22, 23], and dye sensitized TiO_2 [24] are developed for this process. However, the fuel concentration in the products achieved in all the attempts so far is still too low, ranging from 10 ppmV to 1000 ppmV, to be practically useful [1, 4, 5, 7, 8, 11, 12, 15, 16, 18, 20]. For the fuels to be practically useful, the concentration of produced fuels should exceed the lowest combustible concentration of each fuel. For example, for CH_4 and CO, 5.3 vol.% and 12.5 vol.% are required, respectively. Therefore, the big breakthrough in increasing the concentration level is necessary to advance the CO_2 reduction technology.

According to the calculation by the author, the mass transfer time of 10^{*5}–10^{*-1} s is much slower than the photo reaction time of 10^{*-9}–10^{*-15} s in this process. Therefore, the mass transfer is thought to be the main factor contributing to the slow photocatalytic reaction. Another reason causes the low reduction rate is the reoxidization of the products. Namely, due to the reaction surface covered by products, the further movement of the reactants to the reaction surface is prevented and the reverse reaction, that is, re-oxidization, which produces CO_2 from CO and CH_4, occurs. Therefore, it is desirable that the products, that is, CO and CH_4, are removed from the reaction surface as soon as they are produced. The reactants, that is, CO_2 and water vapour, can then continue to react on the reaction surface, and the fuel production can be sustained under this nonequilibrium reaction condition. In other words, by

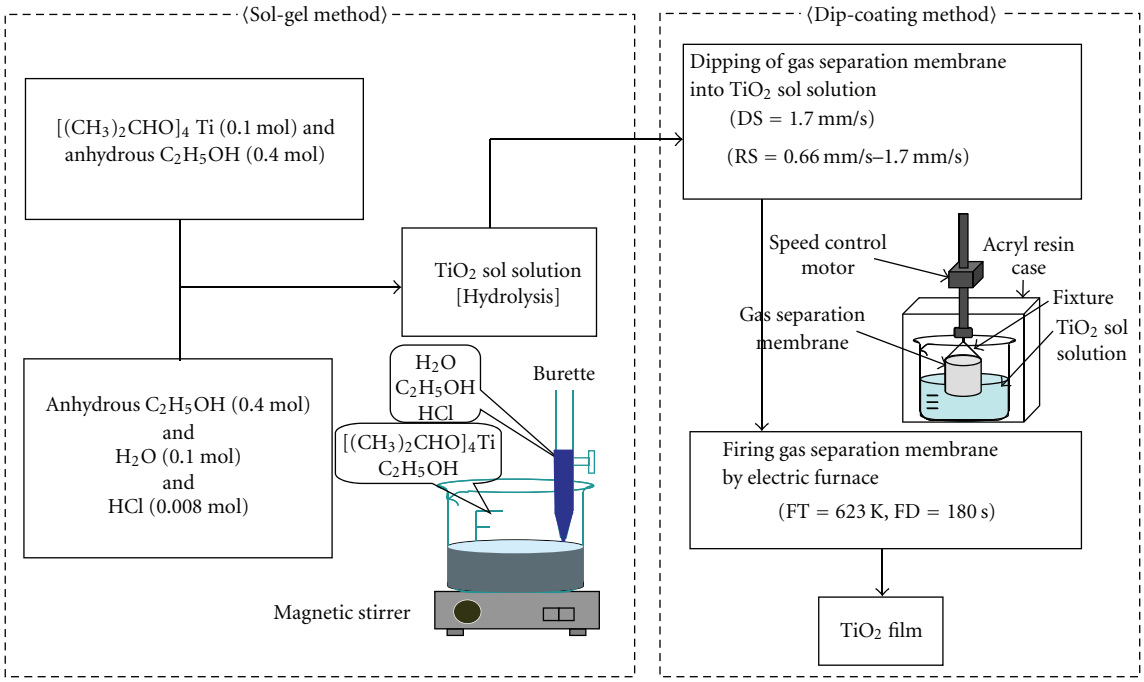

Figure 1: Sol-gel and dip-coating method to prepare TiO_2 film in this study.

removing the products away, the reaction is forced to head to one direction. The gas separation membrane is usually used in the gas separation processes like H_2 production from hydrocarbon, O_2 enrichment from the air, and CO_2 capture of the industrial power plants. Since the molecular diameters of reactants of CO_2 and water vapour are smaller than that of CO and CH_4 (CO_2: 0.33 nm, water vapour: 0.28 nm, CH_4: 0.38 nm, CO: 0.38 nm) [25], the promotion of the reaction by gas separation is thought to be possible and was attempted in this study. This is a novel approach aiming to improve CO_2 reduction performance over the TiO_2. No similar attempts have been reported yet. Therefore, the present paper investigates the effect of preparation condition of membrane reactor consisting of TiO_2 photocatalyst and gas separation membrane and experimental condition on CO_2 reduction performance of the membrane reactor.

2. Experiment

2.1. Preparation of TiO_2 Film Coated on Gas Separation Membrane. Since TiO_2 photocatalyst membrane reactor is a novel approach to improve CO_2 reduction performance over the TiO_2, it is necessary to verify the effect of combination of gas separation membrane and TiO_2 on CO_2 reduction performance. Therefore, the authors investigated the preparation procedure of TiO_2 film coated on gas separation membrane by sol-gel and dip-coating method and the experimental operation conditions to promote the CO_2 reduction performance of the TiO_2 photocatalyst membrane reactor. The rising speed (RS) of gas separation membrane from the TiO_2 sol solution in dip-coating process, which influences the thickness and physical and chemical structure of TiO_2 film coated on gas separation membrane, was investigated. The surface structure and crystallization characteristics of TiO_2 film coated on gas separation membrane, under the various RS conditions, were analysed by SEM (scanning electron microscope), EPMA (electron probe microanalyzer), and XPS (X-ray photoelectron spectroscopy) to understand the impact of difference of RS on the surface structure and crystallization characteristics of TiO_2 film, as the first step. The CO_2 reduction and permeation performance of TiO_2 film coated on gas separation membrane was evaluated by the batch type reactor in order to select the optimal TiO_2 film coating conditions to use to prepare the membrane for the reactor of gas circulation type. In other words, the ideal TiO_2 film for this application should have large reaction surface areas and high crystallization characteristics but does not block the pores in gas separation membrane. After the suitable TiO_2 film coating conditions are known, the CO_2 reduction performance of TiO_2 film coated on porous gas separation membrane was investigated by the gas circulation type reactor. The effectiveness of gas separation and gas circulation using the gas separation membrane on CO_2 reduction performance was compared with the results obtained from the batch type reactor experiment.

Sol-gel and dip-coating method was used for preparing TiO_2 film in this study. Figure 1 shows the flow chart of the sol-gel and dip-coating method. TiO_2 sol solution was made by mixing $[(CH_3)_2CHO]_4Ti$ (purity of 95 wt.%, Nacalai Tesque Co.), anhydrous C_2H_5OH (purity of 99.5 wt.%, Nacalai Tesque Co.), distilled water, and HCl (purity of 35 wt.%, Nacalai Tesque Co.).

The gas separation membrane (silica-alumina gas separation membrane, Noritake Co., Ltd.), which was the porous

Table 1: Physical properties of gas separation membrane.

	Thickness (μm)	Mean pore size (nm)	Void ratio (-)	Permeability (m^2)
(1) Silica (SiO_2) layer	0.2	0.4	0.27	5.44×10^{-22}
(2) γ-alumina (Al_2O_3) layer	2	4	0.44	8.88×10^{-20}
(3) α-alumina (Al_2O_3) layer	100	60	0.39	1.76×10^{-17}
(4) α-alumina (Al_2O_3) supporter	1000	700	0.40	2.45×10^{-15}

Silica layer is the top layer of this gas separation membrane.
γ-alumina layer is the second layer. α-alumina layer is the third layer.
α-alumina supporter is the bottom layer of gas separation membrane.

multilayer ceramic tube, was dipped into TiO_2 sol solution and pulled up at the fixed speed. Then, it was dried out and fired under the controlled firing temperature (FT) and firing duration time (FD), resulting that TiO_2 film was fastened on the surface of gas separation membrane. Coating number (N) was fixed at 1. FT, and FD was set at 623 K and 180 s, respectively. RS varied from 0.66 mm/s to 1.7 mm/s. Downing speed (DS) of gas separation membrane into TiO_2 sol solution in dip-coating process was kept at the constant speed of 1.7 mm/s. Table 1 lists the physical properties of the gas separation membrane. It can be seen from Table 1 that the mean pore size of silica layer is not ideal, as it is not between the molecular diameter of reactants and that of products, as required. It is difficult to find the gas separation membrane with the ideal pore size. However, the gas separation membrane selected is capable of separating gases through both molecular sieving diffusion and so-called Knudsen diffusion mechanisms; therefore, it can be used. The Knudsen diffusion can separate the gases whose molecular diameters are smaller than the pore size of silica layer. Since the molecular diameter of reactant and that of product are actually different as described above, we have decided to adopt this gas separation membrane.

2.2. Experimental Apparatus and Procedure. Figure 2 illustrates the CO_2 reduction reactor that is termed as reactor, with TiO_2 film coated on gas separation membrane. This reactor consists of one gas separation membrane with TiO_2 film (150 mm ($L.$) $\times$ 6 mm ($O.D.$) $\times$ 1 mm ($t.$), whose reaction surface is equal to the outer surface area: 2.26×10^{-3} m^2 and gas filling volume: 2.88×10^{-4} m^3), one quartz glass tube (266 mm ($L.$) $\times$ 42 mm ($O.D.$) $\times$ 2 mm ($t.$)), and four UV lamps (FL16BL/400T16, Raytronics Corp., 400 mm ($L.$) $\times$ 16 mm ($D.$)) located at 20 mm apart from the surface of gas separation membrane symmetrically. These parts are assembled with stainless plates by bolts and nuts. The center wave length and mean light intensity of UV light illuminated from energy UV lamp are 365 nm and 2.4 mW/cm^2, respectively. This is similar to the average light intensity level of UV ray in solar radiation in the daytime.

Figure 3 illustrates the whole experimental system setup, which is termed as membrane reactor. With this membrane reactor, not only batch type but also gas circulation type experiment can be conducted. When it is used for batch type experiment, the valves located at inlet and outlet of reactor are closed. The membrane reactor is composed of reactor part, CO_2 gas cylinder, mass flow controller (MODEL3660, KOFLOC), mass flow meter (CK-1A, KOFLOC), pressure gauge, gas drier, and tube pump (WM-520S/R2, Iwaki Pumps). In the CO_2 reduction experiment by the batch type reactor, CO_2 gas whose purity was 99.995 vol.% was flowed through the reactor as a purged gas for 15 min at first. After that, the valves located at inlet and outlet of reactor were closed. After confirming the gas pressure and gas temperature in the reactor were at 0.1 MPa and 298 K, respectively, the distilled water of 1.00 mL (55.6 mmol) was injected into the reactor, and UV light illumination was started at the same time. This water was vaporized after injected into the reactor. Despite the heat of UV lamp, the temperature in reactor was kept at about 343 K during the CO_2 reduction experiment. The amounts of the injected water and the CO_2 in the batch type reactor are 55.6 mmol and 13.0 mmol, respectively. The gas in reactor was sampled every 24 h in CO_2 reduction experiment. The gas samples were analysed by FID gas chromatograph (GC353B, GL Science) and methanizer (MT221, GL Science). The concentration of water vapour and the temperature in reactor was measured by dew point meter (VAISALA HUMICAP HMT330, VAISALA) and thermocouple, respectively. In this experiment, only CO was detected as the product. In the CO_2 permeation experiment, the CO_2 reduction and permeation experimental system shown in Figure 3 was arranged.

Figure 4 illustrates the CO_2 reduction and permeation experimental system for CO_2 permeation experiment by batch type. In the CO_2 permeation experiment, the CO_2 permeation flux was measured under the condition that the absolute pressure and temperature of supply gas to the apparatus were 0.10–0.40 MPa and 298 K, respectively. The flow rate of supply gas was set at 500 mL/min by mass flow controller. The flow rate of permeation gas was measured by mass flow meter. In the CO_2 reduction experiment carried out by the membrane reactor of gas circulation type, UV light was illuminated under the same condition of batch type reactor until the steady reaction state was confirmed. After that, the gas circulation by tube pump was started. The suction pressure and flow rate of permeation gas were controlled to evaluate the effect of gas separation and circulation on CO_2 reduction performance of this membrane reactor. The suction pressure and flow rate of permeation gas were set at 0.2 MPa and 0.39 mL/min, respectively. The produced CO would be removed from the reactor to outside of the system by switching the outlet valve of reactor on and off when needed. The distilled water of 1.00 mL (55.6 mmol) or 3.00 mL (166.8 mmol) was injected into reactor when the

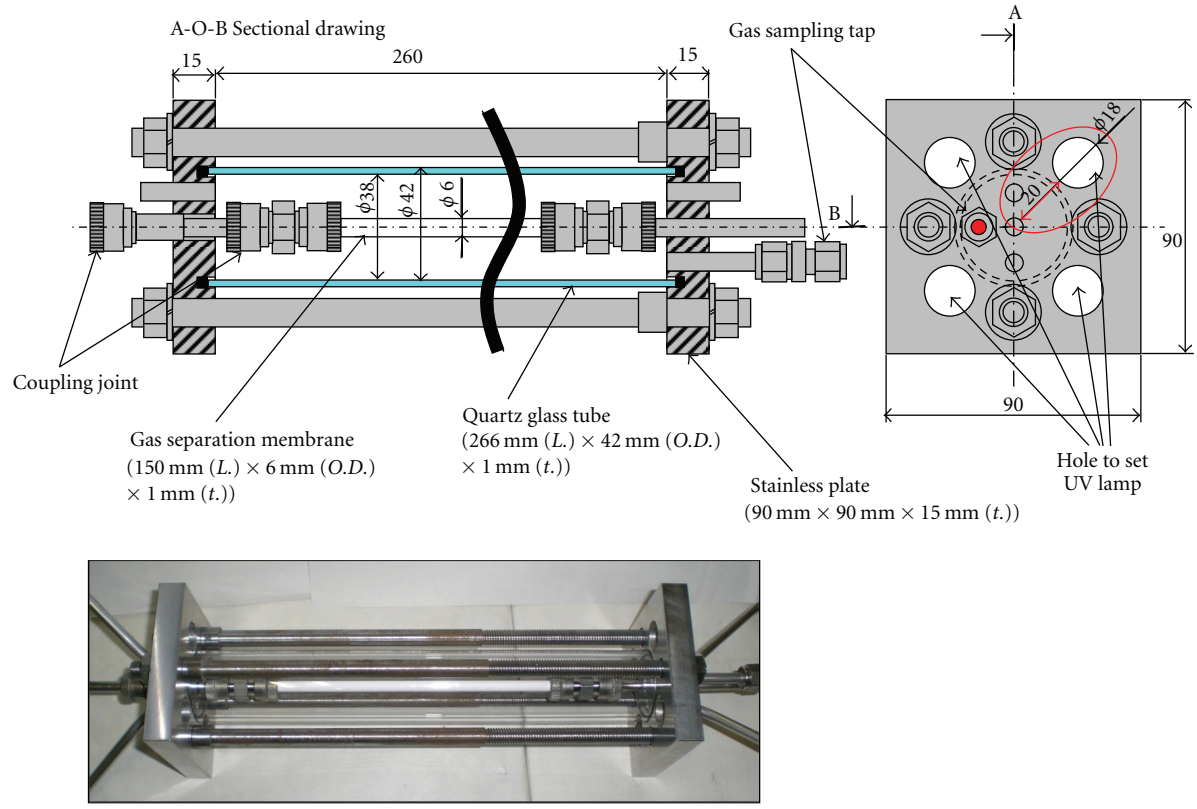

FIGURE 2: CO_2 reduction reactor composed of TiO_2 film coated on gas separation membrane (UV lamp is removed from this figure for understanding the inside of CO_2 reduction reactor).

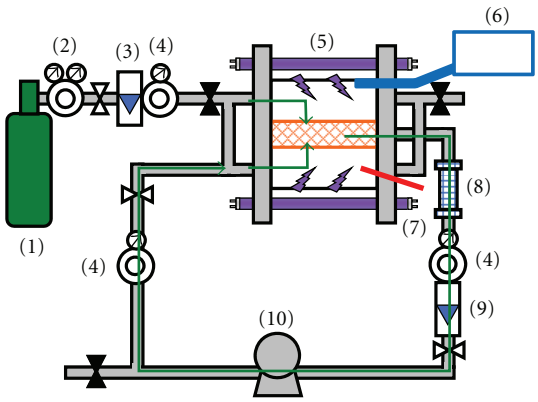

(1) CO_2 gas cylinder (99.995 vol%)
(2) Regulator
(3) Mass flow controller
(4) Pressure gauge
(5) CO_2 reduction reactor
(6) Dew point meter
(7) Thermocouple
(8) Gas drier (Silica gel)
(9) Mass flow meter
(10) Tube pump

FIGURE 3: CO_2 reduction and permeation experiment system.

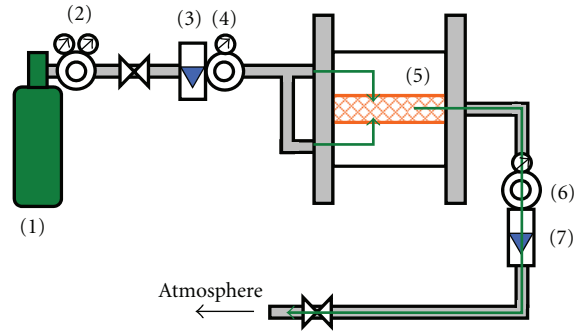

(1) CO_2 gas cylinder
(2) Regulator
(3) Mass flow controller
(4) Pressure gauge
(5) Gas separation membrane
(6) Pressure gauge
(7) Mass flow meter

FIGURE 4: Arranged CO_2 reduction and permeation experimental system for CO_2 permeation experiment.

CO_2 reduction experiment under the condition of batch type reactor was established. The gas samples taken every 24 h from reactor were analysed by FID gas chromatograph and methanizer. The concentration of water vapour and the temperature in the reactor were also measured.

3. Results and Discussion

3.1. Analysis Result of TiO_2 Film Coated on Gas Separation Membrane by SEM. Figures 5 and 6 show SEM images of TiO_2 film prepared under various RS conditions. These SEM images were taken with 200 times and 1500 times magnification under the condition of acceleration voltage is 15 kV and current of $3.0 \times 10^{*-8}$ A. The silica layer covers one-third of surface area of gas separation membrane used

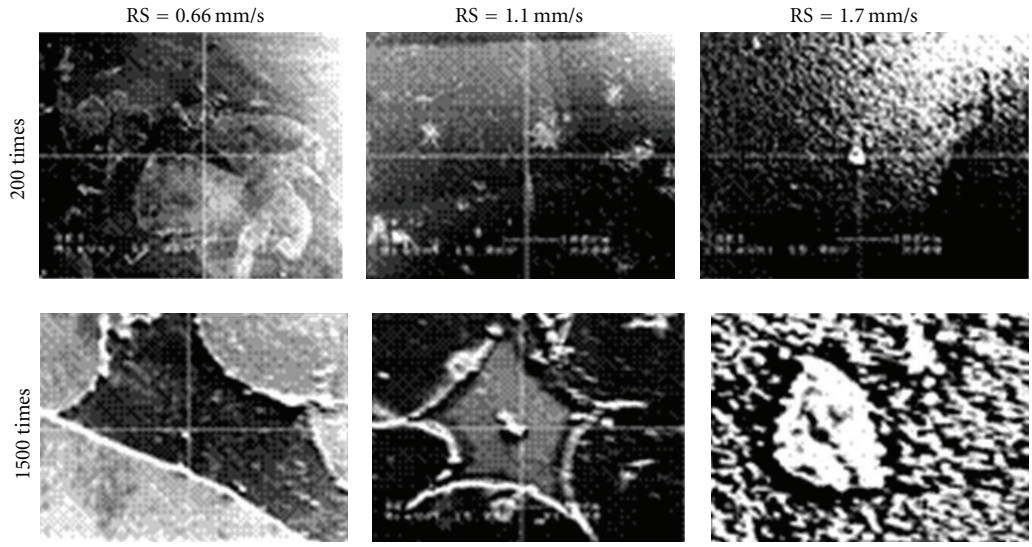

Figure 5: SEM images of TiO_2 film coated on silica layer prepared under various RS conditions.

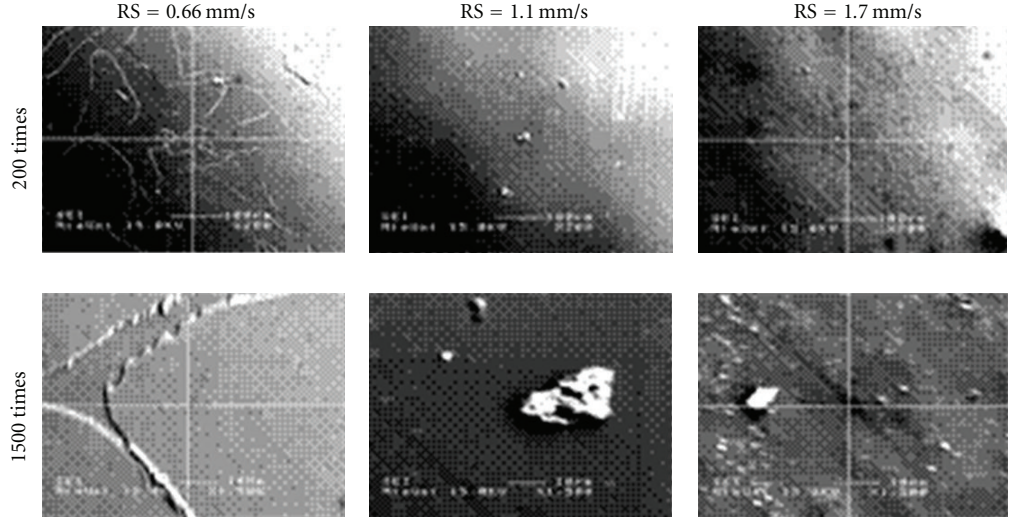

Figure 6: SEM images of TiO_2 film coated on alumina layer prepared under various RS conditions.

in this study at the center, and the alumina layer is exposed except for the area covered by silica layer. Then, SEM images of TiO_2 film coated were taken for the silica-covered area and the alumina area separately. From these figures, it can be seen that the number of clucks of TiO_2 film coated on alumina layer is less than that on silica layer, resulting that the amount of TiO_2 coated on alumina layer is larger than silica layer. Since the pore size of alumina layer is larger than that of silica layer as listed in Table 1, it can be thought that TiO_2 sol solution flows into the alumina layer more easily than the silica layer in dip-coating process. Therefore, it seems that TiO_2 film coated on alumina layer is fixed more strongly than that on silica layer.

3.2. Analysis Result of TiO_2 Film Coated on Gas Separation Membrane by EPMA. Figure 7 demonstrates EPMA images of TiO_2 film prepared under various RS conditions. These EPMA images are taken by 1500 times magnification under the condition of acceleration voltage of 15 kV and current of $3.0 \times 10^{*-8}$ A.

In Figure 7, the concentration distribution of Ti detected in observation area is indicated by the difference of colour. Light colours, for example, white, pink, and red, mean that the amount of Ti is large, while dark colours like black, blue, and green mean that the amount of Ti is small. EPMA detects each element whose crystallization characteristic is memorized in advance. Therefore, if the large concentration of Ti is detected, it means that the amount of crystallized TiO_2 coated on gas separation membrane is large. The average concentration of Ti in the observation area is also shown in Figure 7. According to Figure 7, the average concentration of Ti detected in observation area for alumina

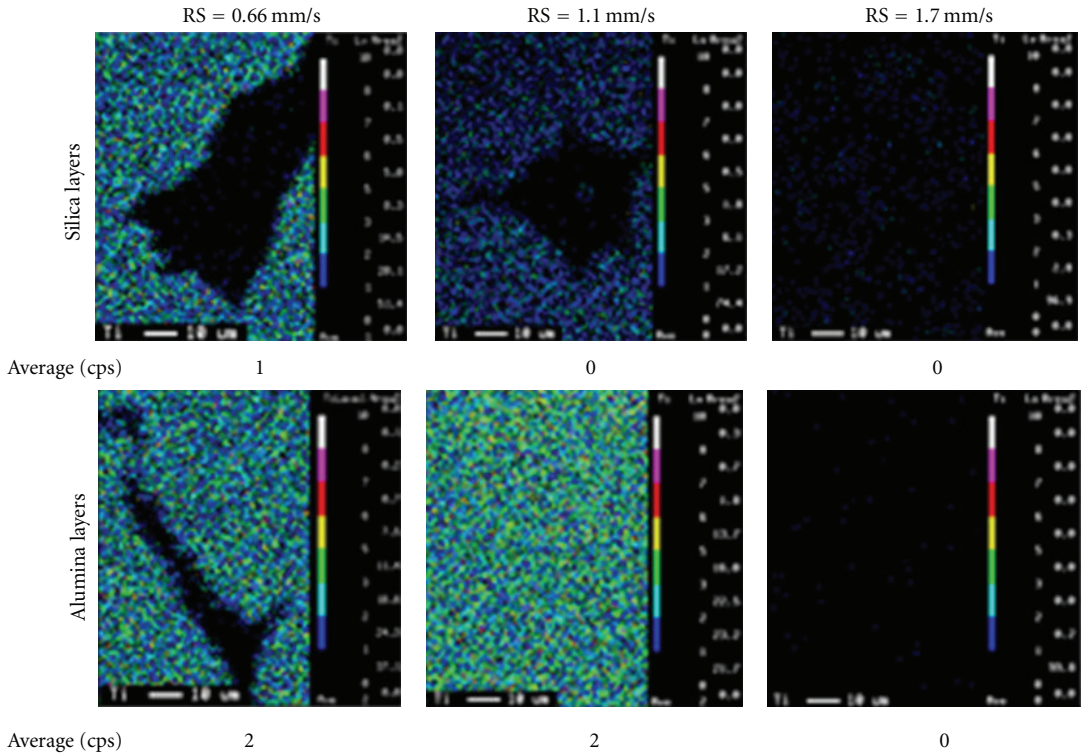

Figure 7: EPMA images of TiO_2 film prepared under various RS conditions.

layer is larger than that for silica layer. It can be said that TiO_2 film is coated in the pores of alumina layer mainly. From Figure 7, it reveals that the concentration of Ti is reduced with the increase in RS. Generally speaking, the thickness of TiO_2 film becomes thick and hubbly with the increase in RS. The thermal stress is acted on the interface between TiO_2 film and gas separation membrane in the firing process, resulting that formation of large clucks and detachment of TiO_2 film occur. Consequently, the concentration of Ti is reduced when RS is high.

3.3. Analysis Result of TiO_2 Film Coated on Gas Separation Membrane by XPS. Figures 8 and 9 show the intensity distributions of Ti detected in silica layer and alumina layer, respectively. These XPS data were obtained under the condition of ion acceleration voltage is 4 kV and pass energy of 112 eV. The samples were sputtered by Ar ion laser whose acceleration voltage is 2 kV. The sputtering speed was 15 nm/min, which was estimated by assuming the sample as SiO_2. The electron orbits of detected elements which were Ti, Si, and Al were set at 2p. From these figures, it is known that the sputtering time for RS = 1.1 mm/s is the shortest among various RS conditions. However, the intensity of detected Ti is over 80000 cps for RS = 1.1 mm/s. It can be said that the amount of Ti is large with RS = 1.1 mm/s, resulting that fine TiO_2 film is prepared. Regarding RS = 0.66 mm/s, it is seen that the intensity of Ti over 60000 cps can be detected up to about sputtering time of 25 min for silica layer. Though the intensity of Ti detected in alumina layer is smaller than that in silica layer, the detecting period of Ti in alumina layer is almost equal to that in silica layer. According to Figure 7, the average concentration of Ti for RS = 0.66 mm/s is the largest among various RS conditions. In addition, when the sputtering time is longer, it can be said that TiO_2 is coated deeper to the thickness direction of gas separation membrane, resulting that the reaction surface of TiO_2 film is larger. From these results, one can conclude that the largest amount of TiO_2 film is coated on gas separation membrane with RS = 0.66 mm/s. Meanwhile, the intensity of detected Ti with RS = 1.7 mm/s is the lowest among various RS conditions. In addition, the average concentration of Ti is 0 cps as shown in Figure 7. Consequently, it is clear that the amount of TiO_2 film coated on gas separation membrane for RS = 1.7 mm/s is very small.

3.4. CO_2 Reduction by the Membrane Reactor of Batch Type. Figure 10 shows the CO concentration change in products with illumination time of UV light for several TiO_2 film prepared under various RS conditions. According to our previous studies, the reversal of superiority or inferiority on CO_2 reduction performance of TiO_2 film among selected parameters was confirmed until UV light illumination time of 48 h. However, this reversal was not confirmed, and the superiority or inferiority among selected parameters was kept after UV light illumination time of 72 h. From this reason, in this study, the data is obtained only up to UV light illumination time of 72 h for the purpose of determining the best condition for promotion of CO_2 reduction

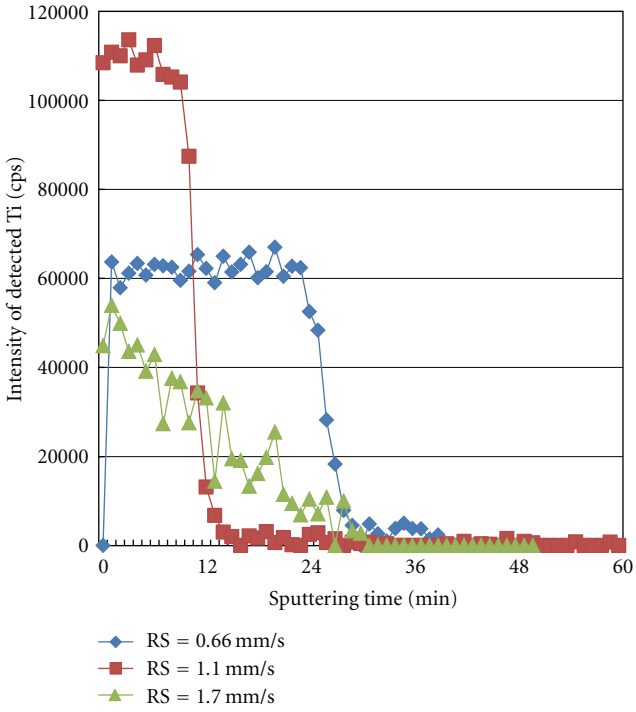

Figure 8: Intensity distributions of detected Ti in silica layer.

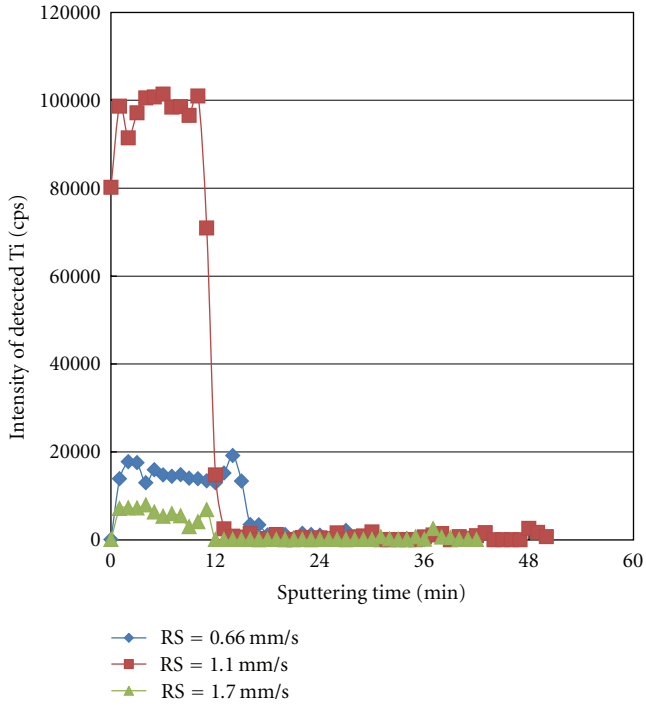

Figure 9: Intensity distributions of detected Ti in alumina layer.

performance. The distilled water of 1.00 mL (55.6 mmol) was injected into reactor at the beginning of the CO_2 reduction experiment.

From the data at UV light illumination time of 72 h shown in Figure 10, it is known that the concentration of CO is increased with decreasing RS values. In this experiment, only CO was detected as a product. Referring to the images of the SEM, EPMA, and XPS shown in Figures 5, 6, 7, 8, and 9, the reason of this is thought to be that the amount of TiO_2 coated on gas separation membrane becomes larger when RS decreases within the range of 0.66–1.7 mm/s. Under slow RS condition, TiO_2 sol solution is easy to remain in the pore of silica and alumina layer in the dip-coating process, and TiO_2 film coated becomes thin and even. Therefore, it is thought that the largest amount of TiO_2 film is coated on gas separation membrane under the condition of RS = 0.66 mm/s.

According to the reaction scheme in this study as shown in Figure 11 [1, 5, 6, 11, 16, 26–29], the number of electron and hydrogen ions (H^+) decides the type of product in the reaction. In this experiment, CH_4, C_2H_4, and the other hydrocarbons were not detected by gas chromatograph, due to less H^+ in the reaction. Therefore, the amount of water vapour injected into the reactor is an important parameter to be investigated since it is the source of H^+. From the reaction scheme, water vapour of 1 mol to CO_2 of 1 mol is necessary to produce CO of 1 mol. In this experiment, the amount of substance of injected water and CO_2 charged in the batch type reactor is 55.6 mmol and 13.0 mmol, respectively, resulting that the molar ratio of water vapour to CO_2 is 4.28. Although the amount of water vapour injected seemed sufficient for this reaction, the change in temperature distribution and the concentration distribution of water vapour in the batch type reactor with time need to be checked to confirm what had happened.

3.5. CO_2 Permeation by the Membrane Reactor of Batch Type. Figure 12 shows the relationship between CO_2 permeation flux and pressure difference for several TiO_2 film prepared under various RS conditions. The pressure difference is known by subtracting the gas pressure after penetrating the gas separation membrane from the gas pressure before. The CO_2 permeation flux is calculated by the following equation:

$$F_{CO_2} = \frac{V_p}{A_p t_p}, \tag{1}$$

where F_{CO_2}, V_p, A_p, and t_p are CO_2 permeation flux [mol/(m^2·s)], volume of permeated gas (mol), outer surface area of gas separation membrane (m^2), and gas separation time (s), respectively.

Comparing these results at pressure difference of 0.30 MPa, it is known that the CO_2 permeation flux for RS = 1.1 mm/s is the highest among these RS conditions. According to XPS analysis as shown in Figures 8 and 9, the sputtering time of detecting Ti for RS = 1.1 mm/s is the shortest among various RS conditions, indicating that the depth of coated TiO_2 film diffused into the silica and alumina layers of gas separation membrane is the shallowest. Consequently, the highest CO_2 permeation flux is obtained at RS = 1.1 mm/s. On the other hand, regarding RS = 0.66 mm/s and 1.7 mm/s, the sputtering time of detecting Ti is longer though the intensity of Ti detected is lower as shown

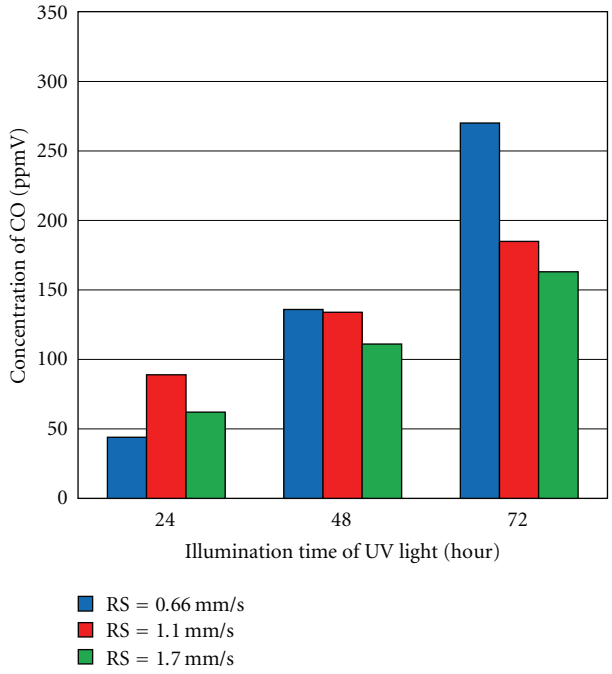

Figure 10: Concentration change in produced CO with illumination time of UV light for several TiO_2 film prepared under conditions of different RS.

in Figures 8 and 9, indicating the depth of coated TiO_2 film. TiO_2 film diffused into the silica and alumina layers is deeper, thus the CO_2 permeation flux is lower.

3.6. Selection of the Optimum Coating Condition. To select the optimum coating condition of TiO_2 film which would lead to the highest CO_2 reduction and permeation performance, the results by SEM and EPMA analysis and the results of CO_2 reduction and permeation experiment by the batch type reactor are compared and analysed. Figure 13 shows the comparison of the results between the concentration of produced CO and the CO_2 permeation flux for various RS conditions. In Figure 13, the concentration of CO at UV illumination of 72 h shown in Figure 10 and CO_2 permeation flux at pressure difference of 0.30 MPa shown in Figure 12 are demonstrated. It can be seen that the concentration of CO is decreased with increasing RS gradually. On the other hand, the CO_2 permeation flux peaks at RS = 1.1 mm/s. Therefore, the optimum RS is different from the viewpoint of CO_2 reduction and permeation performance. Since the main goal of this study is to promote the CO_2 reduction performance, we have selected the RS = 0.66 mm/s as the optimum coating condition to reduce CO_2.

3.7. CO_2 Reduction by the Membrane Reactor of Gas Circulation Type. According to the reaction scheme shown in Figure 11, CO is reoxidized with the O_2, that is, a by-product in this reaction. After attaining to the steady reaction state, the concentration of CO is decreased. This is the opposite reaction toward CO_2 reduction into fuel. Moreover, since the

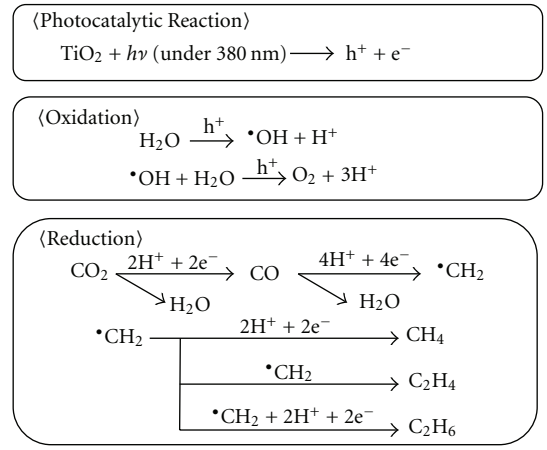

Figure 11: Reaction scheme of CO_2 reduction into fuel by TiO_2 photocatalyst.

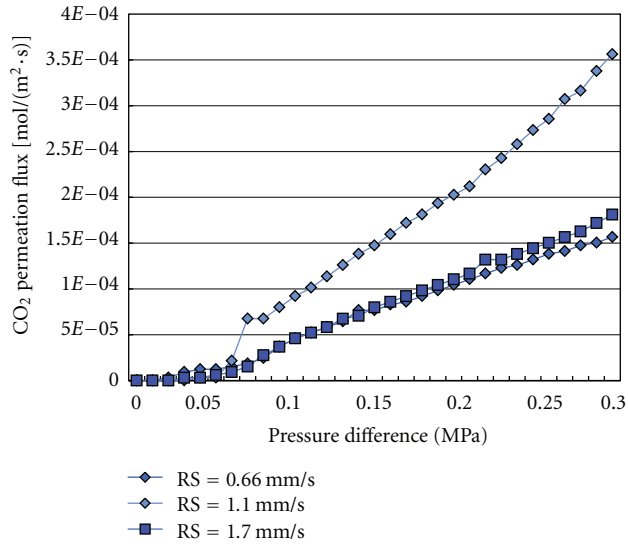

Figure 12: Relationship between CO_2 permeation flux and pressure difference for several TiO_2 film prepared under various RS conditions.

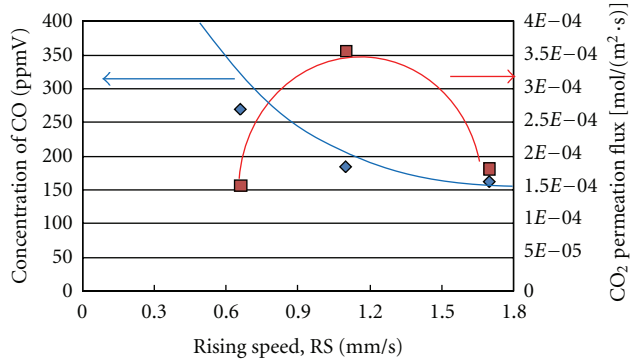

Figure 13: Comparison of the results between concentration of produced CO and CO_2 permeation flux for each condition.

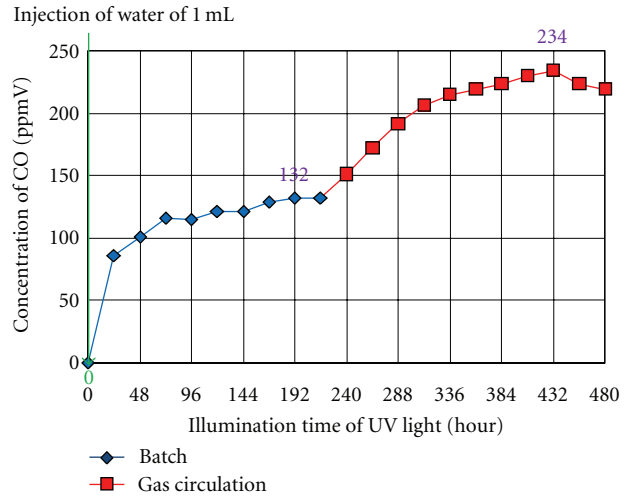

Figure 14: Concentration change in produced CO with illumination time of UV light (injection of water of 1.00 mL at the start of CO_2 reduction experiment).

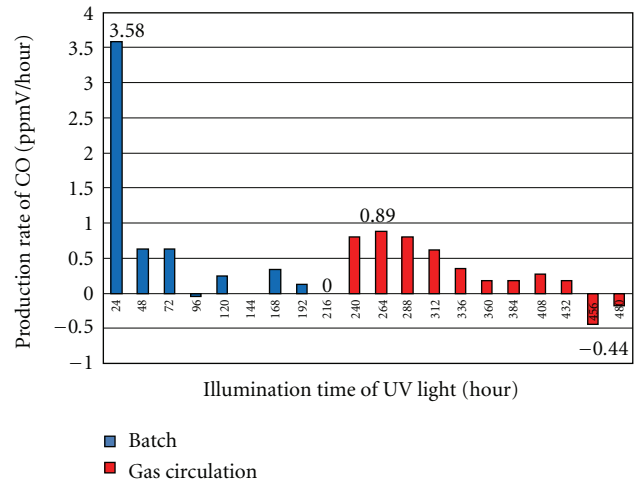

Figure 15: Change in production rate of CO with illumination time of UV light (injection of water of 1.00 mL at the start of CO_2 reduction experiment).

photocatalytic reaction occurred on the reaction surface, it is easy for the reaction surface to be covered by the products, which would stop the further reaction to happen. Therefore, removing the product of CO and CH_4 from the reaction surface as well as transporting the reactants, that is, CO_2 and water vapour, to the reaction surface quickly are necessary to promote further reaction and prevent the re-oxidization of CO. In this study, a tube pump and a gas separation membrane are used to realize this desirable measure for the promotion of CO_2 reduction performance.

Figure 14 shows the concentration change of CO produced with illumination time of UV light. In this experiment, only CO was detected as a product. The distilled water of 1.00 mL (55.6 mmol) was injected into reactor when the CO_2 reduction experiment by batch type reactor started. To show the effect of gas separation and circulation on the CO_2 reduction performance, the gas circulation by tube pump only starts after the steady reaction state is reached. The steady reaction state was defined as the state at which the concentration of CO no longer increases along the time. Since the concentration of CO is diluted with the CO_2 in the pipe lines of the gas circulation type reactor after starting gas circulation, the concentration of CO is corrected by the following equation:

$$C_c = \frac{V_{\text{total}} C_d}{V_{\text{batch}}}, \tag{2}$$

where C_c, V_{total}, C_d, and V_{batch} mean corrected concentration of CO (ppmV), total gas volume inside the experimental apparatus including the gas volume in the pipe lines (m^3), detected concentration of CO (ppmV), and total gas volume inside the experimental apparatus in the case of batch type reactor (m^3), respectively. The experiment by batch type and gas circulation type was carried out during the period from 0 h to 216 h and from 216 h to 480 h, respectively.

It is observed that the concentration of CO in the reactor keeps increasing until 72 h and starts to be steady after 72 h in the experiment by batch type reactor. The highest concentration of CO which is 132 ppmV is obtained at 192 h after illuminating UV light. Since the concentration of CO is not increased over 192 h, it is determined that the experiment by batch type reactor reaches the steady reaction state at 192 h. After gas circulation, the concentration of CO starts to increase again and peaks at 234 ppmV at UV light illumination of 432 h, which demonstrated the positive effect of gas separation and circulation on CO_2 reduction performance. To show that the steady reaction state and inverse reaction have occurred or not clearly, the change in production rate of CO with illumination time of UV light is shown in Figure 15. Production rate of CO can classify the reaction state into progressive, steady, and inverse reaction state by positive, 0, and negative value, respectively. The production rate of CO, in Figure 15, is calculated by

$$R_{\text{CO}} = \frac{C_C}{t_{\text{int}}}, \tag{3}$$

where R_{CO} and t_{int} mean production rate of CO (ppmV) and gas sampling interval (h), respectively. The R_{CO} used for calculating is 24 h.

In the experiment by batch type reactor, it can be seen that the production rate of CO peaks at 3.58 ppmV/h at the UV light illumination time of 24 h and is decreased afterwards gradually. The production rate of CO which is 0 means that the reaction steady state is reached. The negative value of the production rate means the inverse reaction, that is, re-oxidization occurs. In the experiment by gas circulation type reactor, the production rate of CO after starting the gas circulation peaks at the highest value of 0.89 ppmV/h in the period from 240 h to 264 h. However, the production rate of CO became smaller after the passage time of 48 h, that is, after the total illumination time of UV light of 264 h. Comparing the production rate of CO after starting the gas circulation and that at steady state of batch type reactor except for the period from 0 h to 24 h, the effect of gas

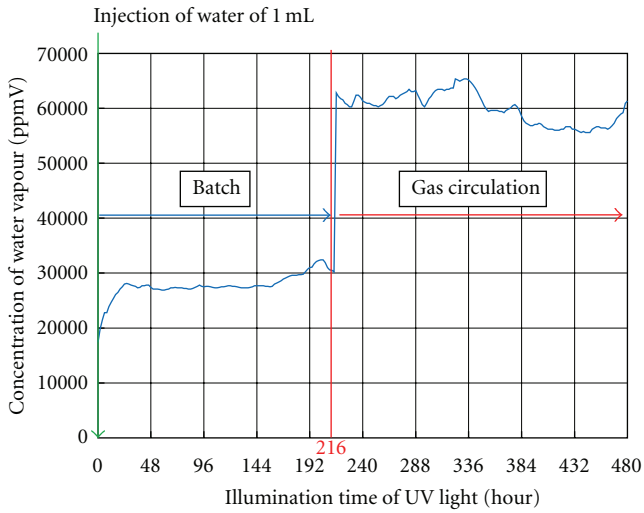

Figure 16: Concentration change in water vapour during the CO_2 reduction experiment by batch type and gas circulation type reactor with illumination time of UV light (injection of water of 1.00 mL at the start of CO_2 reduction experiment).

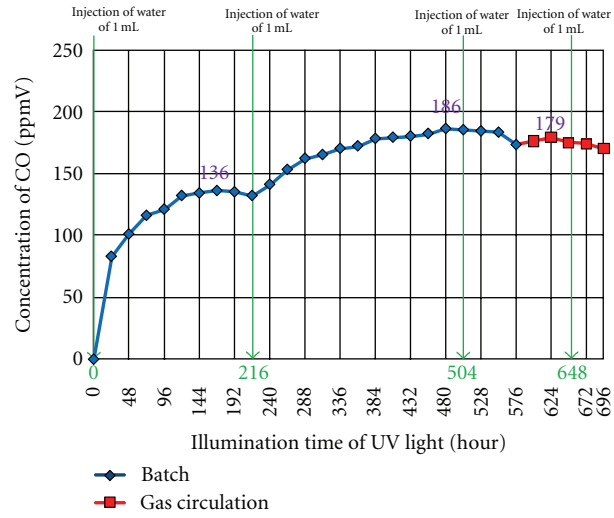

Figure 17: Concentration change in produced CO with illumination time of UV light (injection of water of 1.00 mL many times).

separation and circulation on CO_2 reduction can be verified. However, the production rate of CO and the concentration of CO are still lower than the target value levels set for this study. Figure 16 shows the concentration of the water vapour during the CO_2 reduction experiment by batch type and gas circulation type reactor with illumination time of UV light. Since the concentration of water vapour is diluted with the gas in the pipe lines of the gas circulation type reactor after starting gas circulation, the concentration of water vapour is corrected by the following equation:

$$C_{c\text{-}H_2O} = \frac{V_{\text{total}} C_{d\text{-}H_2O}}{V_{\text{batch}}}, \tag{4}$$

where $C_{c\text{-}H_2O}$, V_{total}, $C_{d\text{-}H_2O}$, and V_{batch} mean corrected concentration of water vapour (ppmV), total gas volume inside the experimental apparatus including the gas volume in the pipe lines (m^3), measured concentration of water vapour (ppmV), and total gas volume inside the experimental apparatus in the case of batch type reactor (m^3), respectively. From this figure, it is known that the highest concentration of water vapour in the experiment by batch type reactor and gas circulation reactor is 32400 ppmV and 65387 ppmV, respectively. According to saturated steam table, if the water vapour is saturated in the reactor at 343 K, it should have the concentration of 307545 ppmV. The 1.00 mL water injected into batch type reactor and gas circulation reactor, if all evaporated, could make the vapour concentration of 53040 ppmV and 112968 ppmV, theoretically. As not sure the lower water concentration measured in caused by water vapour was absorbed by gas separation membrane or not all of water injected was vaporized, more water was injected in order to evaluate the effect of amount and timing of water injection.

The further experiment plan was based on the assumption that at the steady and inverse reaction states, there was not sufficient water in the system. Therefore, the water was injected into reactor when the steady and inverse reaction state in the CO_2 reduction was confirmed for not only batch type but also gas circulation type experiment. The amount of water injected was 1.00 mL at every time in this experiment. If the steady state was maintained after the injection of water in the batch type experiment by reactor, the gas circulation experiment then starts.

Figure 17 shows the concentration change in produced CO with illumination time of UV light. The initial distilled water of 1.00 mL (55.6 mmol) was injected into reactor when the CO_2 reduction experiment by batch type reactor started. It had shown that the concentration of CO in the batch type reactor kept increasing until 168 h, and the concentration of CO reached 136 ppmV. After the water of 1.00 mL was added into reactor at 216 h when the steady state was confirmed, the concentration of CO increased again and attained to 186 ppmV at 480 h. Since the steady state was confirmed again at 504 h, another 1.00 mL of water was added into reactor again. However, the concentration of CO did not increase any more, indicating the steady state maintained. After gas circulation started from 576 h, the concentration of CO started to increase again and peaked at 179 ppmV at total UV light illumination of 624 h. Since the steady state in the experiment by gas circulation type reactor was confirmed at 648 h, the further 1.00 mL of water was injected into reactor. However, the concentration of CO did not increase further, indicating the water inside system was sufficient, and its effect was peaked.

Figure 18 shows the concentration change in water vapour inside the system in the water adding experiment described above. From this figure, the measured concentration of water vapour obtained in CO_2 reduction experiment by batch type reactor is almost 25000 ppmV with total 3.00 mL water injected.

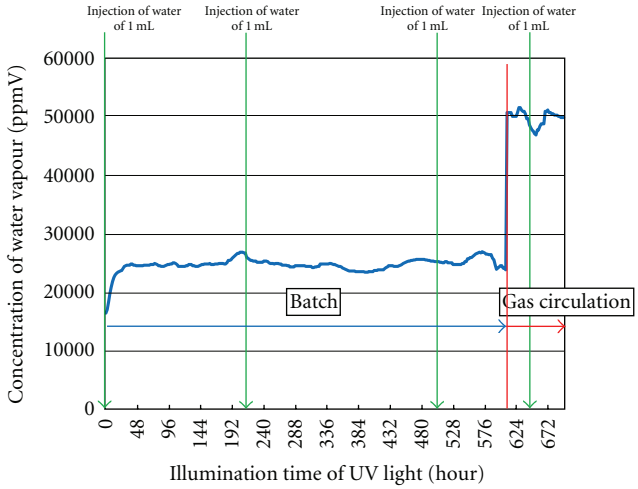

Figure 18: Concentration change in water vapour during the CO_2 reduction experiment by batch type and gas circulation type reactor with illumination time of UV light (injection of water of 1.00 mL many times).

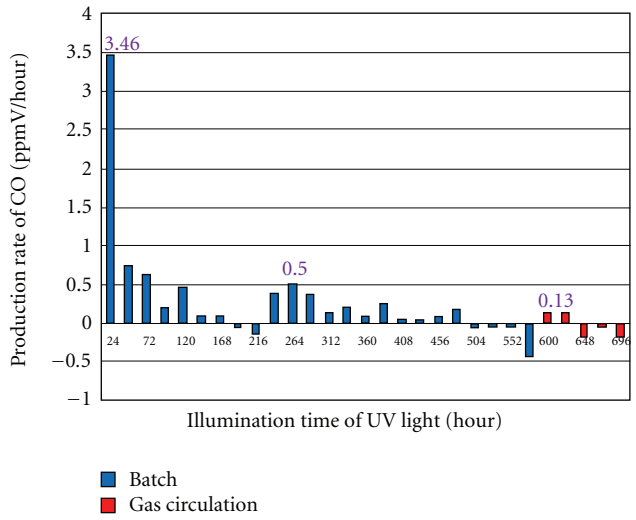

Figure 19: Change in production rate of CO with illumination time of UV light (injection of water of 1.00 mL many times).

Figure 19 shows the change in production rate of CO with illumination time of UV light. From this figure, it can be seen that there are two peaks of production rate of CO in CO_2 reduction experiment by batch type reactor, and there is one peak of production rate of CO in CO_2 reduction experiment by gas circulation type. The first peak was obtained at UV light illumination of 24 h with total of 1.00 mL water in the system, which was injected at the start of CO_2 reduction experiment. According to Figure 20, the production rate of CO decreases, after peaking at 24 h, gradually and reaches negative value at UV light illumination of 216 h. As mentioned above, since the steady reaction state was confirmed at UV light illumination of 216 h, the other 1.00 mL water was added into reactor. As a result, the second peak was obtained at UV light illumination of

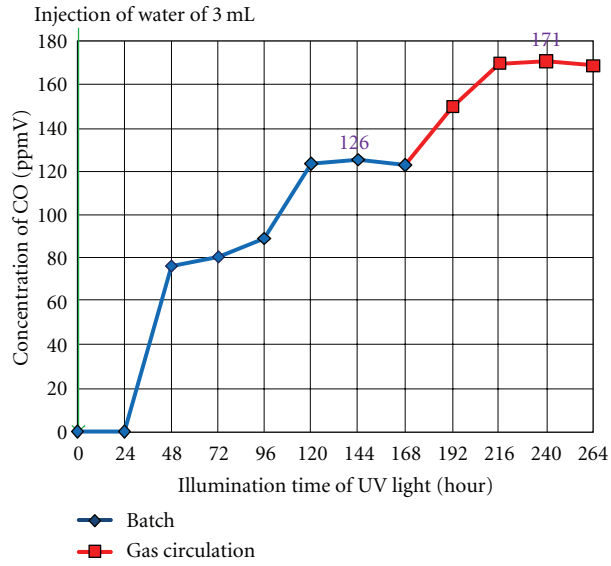

Figure 20: Concentration change in produced CO with illumination time of UV light (injection of water of 3.00 mL at the start of CO_2 reduction experiment).

264 h. After that, the production rate of CO decreases again. Although further 1.00 mL water was added into reactor again at UV light illumination of 504 h, the production rate of CO remains negative value. After gas circulation from total UV light illumination of 576 h, the production rate of CO increases and peaks at total UV light illumination of 600 h. From these results, the effect of water injection on the promotion of CO_2 reduction performance is verified. However, both the highest concentration and the highest production rate of CO in this CO_2 reduction experiment are lower than those in the case of only total 1.00 mL water injected. In addition, compared to the case of total amount of water injected of 1.00 mL, the effect of switching batch type reactor to gas circulation type reactor on the promotion of CO_2 reduction performance is not confirmed in this experiment.

Nevertheless, the above-described results seem to reveal that the optimum timing of water injection is the very beginning of CO_2 reduction experiment. Therefore, one more experiment was conducted, that is, the distilled water of 3.00 mL (166.8 mmol) was injected into reactor at the very beginning of the experiment. Figure 20 shows the concentration change in produced CO with illumination time of UV light. The experiment by batch type and gas circulation type reactor was carried out during the period from 0 h to 168 h and from 168 h to 264 h, respectively. The highest concentration of CO which is 126 ppmV is obtained at UV light illumination of 144 h. Since the concentration of CO is not increased over 144 h, indicating that the experiment by batch type reactor attains to the steady reaction state, the gas circulation was started. After gas circulation, the concentration of CO starts to increase again and peaks at 171 ppmV at UV light illumination of 240 h.

Figures 21 and 22 show the comparison in production rate of CO and change rate of water vapour with illumination

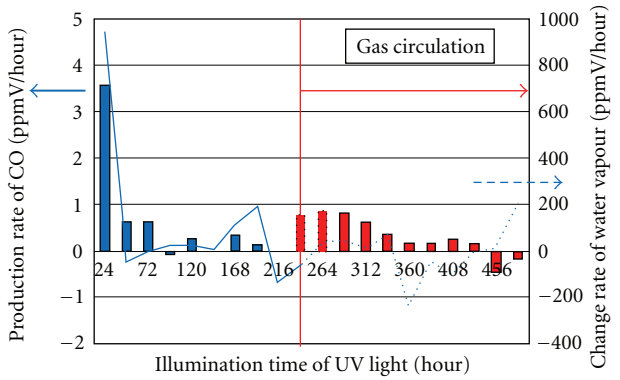

FIGURE 21: Change in production rate of CO and change rate of water vapour with illumination time of UV light for the amount of water injected of 1.00 mL.

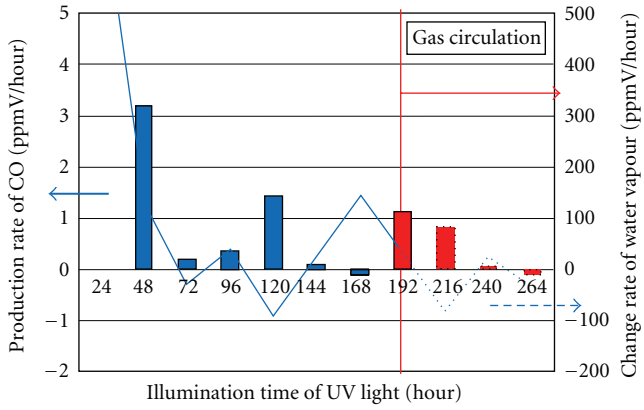

FIGURE 22: Change in production rate of CO and change rate of water vapour with illumination time of UV light for the amount of water injected of 3.00 mL.

time of UV light for the amount of water injected of 1.00 mL and that of 3.00 mL, respectively. The change rate of water vapour is calculated by

$$R_{H_2O} = \frac{\Delta C_{H_2O}}{t_{int}}, \tag{5}$$

where R_{H_2O}, ΔC_{H_2O}, and t_{int} mean change rate of water vapour (ppmV/hour), the amount of increase in concentration of water vapour (ppmV), and measurement interval of water vapour (h), respectively. The used for calculating R_{H_2O} is 24 h.

From these figures, it can be seen that the concentration of water vapour in both cases decreases rapidly from 0 h to 48 h. Since the highest production rates of CO for the amount of water injected of 1.00 mL and 3.00 mL are obtained from 0 h to 48 h, the CO_2 reduction is carried out well in the period. While the concentration of water vapour increases with illumination time of UV light from 0 h to 24 h due to temperature rise in reactor, the change rate of water vapour closes to 0 in the period from 48 h to 96 h irrespective of the amount of water injected. Therefore, it can be thought that the amount of water consumed by photocatalytic reaction is balanced out by the amount of water vaporized due to the heat of UV lamp in the period from 48 h to 96 h. After starting gas circulation, the change rate of water vapour keeps at low level and decreases gradually irrespective of the amount of water injected, while the production rate of CO rises. Since the CO_2 reduction performance is promoted by gas separation and circulation operation, the water vapour is consumed by the oxidization reaction shown in Figure 11. In addition, the water vapour is also adsorbed by drier, which is installed to protect the mass flow meter, in pipeline of gas circulation type reactor during gas circulation. The water concentration increase due to temperature increase balances out by consumption of both oxidization reaction and adsorption by drier. Therefore, the change rate of water vapour keeps low and decreases gradually after starting gas circulation. Consequently, it reveals that CO_2 reduction performance of gas circulation type reactor is declined by increasing the amount of water injected due to decreasing the concentration of water vapour.

Therefore, it can be concluded that too much water in that system, no matter when it was added, would not help improving the CO_2 reduction performance.

Finally, the conversion and the quantum yield are calculated for the best result, which was obtained under the condition that the distilled water of 1.00 mL was injected into reactor when the CO_2 reduction experiment by batch type reactor started, in gas circulation experiment of this study. In this study, the conversion is calculated by the following equation:

$$\alpha = \frac{C_C}{C_{CO_2\text{-}0}} \times 100, \tag{6}$$

where α is the conversion (%), $C_{CO_2\text{-}0}$ is the concentration of CO_2 in the reactor and pipelines at the start of CO_2 reduction experiment (ppmV). In this study, CO of 1 mol is produced from CO_2 of 1 mol according to reduction reaction in the reaction scheme shown in Figure 11. Then, it is thought that C_C is equivalent to the amount of concentration of CO_2 decreased by reduction reaction. From (6), the conversion under the best result condition is calculated as follows:

$$\alpha = \frac{(234)}{(99.995 \times 10000)} \times 100 = 0.0234\ (\%). \tag{7}$$

On the other hand, the quantum yield is calculated by the following equation in this study:

$$\eta = \frac{N_{output}}{N_{input}} \times 100,$$

$$N_{input} = \frac{I \times t \times \lambda \times A_{re}}{h \times c}, \tag{8}$$

$$N_{output} = N_{CO} M_{CO} N_A = N_{CO} \times \frac{V_{total} \times C_C}{V_{CO\text{-}mol}} \times N_A,$$

where η is the quantum yield (%), N_{input} is the number of photon absorbed by TiO_2 photocatalyst (-), N_{output} is the number of photon used for photocatalytic reaction (-), I is the light intensity of UV light (W/cm^2), t is the UV light

illumination time (s), λ is the wave length limit of light which TiO_2 absorbs for photocatalytic reaction (m), A_{re} is the reaction surface area of TiO_2 film which is thought to be almost equal to outer surface area of gas separation membrane (cm^2), h is Plank's constant (J·s), c is light speed (m/s), N_{CO} is the electron number which is necessary for producing CO of a molecular (-), M_{CO} is the amount of substance of produced CO (mol), N_A is Avogadro's number (1/mol), V_{total} is the total gas volume inside the experimental apparatus including the gas volume in the pipe lines (m^3), $V_{CO\text{-}mol}$ is the volume of CO of a mol at initial temperature in experimental apparatus (m^3). From these equations, the quantum yield under the best result condition is calculated as follows:

$$
\begin{aligned}
&N_{\text{input}} \\
&\quad = \frac{(2.4\times10^{-3})\times(432\times3600)\times(380\times10^{-9})\times(28.3)}{(6.63\times10^{-34})\times(3.00\times10^{8})} \\
&\quad = 2.02\times10^{23}, \\
&N_{\text{output}} \\
&\quad = (2)\times\frac{(6.56\times10^{-7})\times(234\times10^{-6})}{(8.76\times10^{-7})}\times(6.02\times10^{23}) \\
&\quad = 2.11\times10^{20}, \\
&\eta = \frac{(2.11\times10^{20})}{(2.02\times10^{23})}\times100 = 0.105\ (\%).
\end{aligned}
\tag{9}
$$

Since the conversion and the quantum yield are low, further investigation, for instance, controlling the TiO_2 film structure coated on gas separation membrane and metal doping which lead promotion of reduction reaction are necessary. They are future subjects in this study.

4. Conclusions

Based on the above-experimental results and discussion, the following conclusions can be drawn from this experimental study.

According to characterization by SEM, EPMA, and XPS, the amount of TiO_2 film coated on gas separation membrane is reduced with increasing RS, and the largest amount of TiO_2 film is obtained for RS = 0.66 mm/s among various RS conditions investigated in this study.

According to CO_2 reduction experiment by batch type reactor, the concentration of CO is decreased with increasing RS gradually. On the other hand, the CO_2 permeation flux peaks at RS = 1.1 mm/s. Since the main goal of this study is to promote the CO_2 reduction performance, the RS = 0.66 mm/s is selected as the optimum coating condition in this study.

According to CO_2 reduction experiment by gas circulation type reactor, the positive effect of gas separation and circulation on CO_2 reduction performance is confirmed. However, too much water in that system which cannot be consumed in CO_2 reduction process, no matter when it was added, would not help improving the CO_2 reduction performance.

References

[1] K. Adachi, K. Ohta, and T. Mizuno, "Photocatalytic reduction of carbon dioxide to hydrocarbon using copper-loaded titanium dioxide," *Solar Energy*, vol. 53, no. 2, pp. 187–190, 1994.

[2] M. Anpo and K. Chiba, "Photocatalytic reduction of CO_2 on anchored titanium oxide catalysts," *Journal of Molecular Catalysis*, vol. 74, no. 1–3, pp. 207–212, 1992.

[3] B. Aurian-Blajeni, M. Halmann, and J. Manassen, "Photoreduction of carbon dioxide and water into formaldehyde and methanol on semiconductor materials," *Solar Energy*, vol. 25, no. 2, pp. 165–170, 1980.

[4] G. R. Dey, A. D. Belapurkar, and K. Kishore, "Photo-catalytic reduction of carbon dioxide to methane using TiO_2 as suspension in water," *Journal of Photochemistry and Photobiology, A*, vol. 163, no. 3, pp. 503–508, 2004.

[5] K. Hirano, K. Inoue, and T. Yatsu, "Photocatalysed reduction of CO_2 in aqueous TiO_2 suspension mixed with copper powder," *Journal of Photochemistry and Photobiology, A*, vol. 64, no. 2, pp. 255–258, 1992.

[6] T. Inoue, A. Fujishima, S. Konishi, and K. Honda, "Photoelectrocatalytic reduction of carbon dioxide in aqueous suspensions of semiconductor powers," *Nature*, vol. 277, no. 5698, pp. 637–638, 1979.

[7] O. Ishitani, C. Inoue, Y. Suzuki, and T. Ibusuki, "Phootcatalytic reduction of carbon dioxide to methane and acetic acid by an aqueous suspension of metal-deposited TiO_2 ," *Journal of Photochemistry and Photobiology, A*, vol. 72, pp. 269–271, 1993.

[8] S. Kaneco, H. Kurimoto, Y. Shimizu, K. Ohta, and T. Mizuno, "Photocatalytic reduction of CO_2 using TiO_2 powders in supercritical fluid CO_2 ," *Energy*, vol. 24, no. 1, pp. 21–30, 1999.

[9] K. Ogura, M. Kawano, J. Yano, and Y. Sakata, "Visible-light-assisted decomposition of H_2O and photomethanation of CO_2 over CeO_2TiO_2 catalyst," *Journal of Photochemistry and Photobiology, A*, vol. 66, no. 1, pp. 91–97, 1992.

[10] K. Takeuchi, S. Murasawa, and T. Ibusuki, *World of Photocatalyst*, Kougyouchousakai, Tokyo, Japan, 2001.

[11] Z. Goren, I. Willner, A. J. Nelson, and A. J. Frank, "Selective photoreduction of CO_2/HCO_3^- to formate by aqueous suspensions and colloids of Pd-TiO_2 ," *Journal of Physical Chemistry*, vol. 94, no. 9, pp. 3784–3790, 1990.

[12] M. Halmann, V. Katzir, E. Borgarello, and J. Kiwi, "Photoassisted carbon dioxide reduction on aqueous suspensions of titanium dioxide," *Solar Energy Materials*, vol. 10, no. 1, pp. 85–91, 1984.

[13] T. Ibusuki, "Reduction of CO_2 by Photocatalyst," *Syokubai*, vol. 35, pp. 506–512, 1993.

[14] K. Kawano, T. Uehara, H. Kato, and K. Hirano, "Photocatalysed reduction of CO_2 in aqueous TiO_2 suspension mixed with various metal powder," *Kagaku to Kyoiku*, vol. 41, pp. 766–770, 1993.

[15] C. C. Lo, C. H. Hung, C. S. Yuan, and J. F. Wu, "Photoreduction of carbon dioxide with H_2 and H_2O over TiO_2 and ZrO_2 in a circulated photocatalytic reactor," *Solar Energy Materials and Solar Cells*, vol. 91, no. 19, pp. 1765–1774, 2007.

[16] I. H. Tseng, W. C. Chang, and J. C. S. Wu, "Photoreduction of CO_2 using sol-gel derived titania and titania-supported copper catalysts," *Applied Catalysis B*, vol. 37, no. 1, pp. 37–48, 2002.

[17] H. Yamashita, H. Nishiguchi, N. Kamada, and M. Anpo, "Photocatalytic Reduction of CO_2 with H_2O on TiO_2 and Cu/TiO_2 Catalysts," *Research on Chemical Intermediates*, vol. 20, pp. 815–823, 1994.

[18] P. Pathak, M. J. Meziani, Y. Li, L. T. Cureton, and Y. P. Sun, "Improving photoreduction of CO_2 with homogeneously dispersed nanoscale TiO_2 catalysts," *Chemical Communications*, vol. 10, no. 10, pp. 1234–1235, 2004.

[19] J. Qu, X. Zhang, Y. Wang, and C. Xie, "Electrochemical reduction of CO_2 on RuO_2/TiO_2 nanotubes composite modified Pt electrode," *Electrochimica Acta*, vol. 50, no. 16-17, pp. 3576–3580, 2005.

[20] X. H. Xia, Z. J. Jia, Y. Yu, Y. Liang, Z. Wang, and L. L. Ma, "Preparation of multi-walled carbon nanotube supported TiO_2 and its photocatalytic activity in the reduction of CO_2 with H_2O," *Carbon*, vol. 45, no. 4, pp. 717–721, 2007.

[21] F. Cecchet, M. Alebbi, C. A. Bignozzi, and F. Paolucci, "Efficiency enhancement of the electrocatalytic reduction of CO_2: fac-[Re(v-bpy)$(CO)_3$Cl] electropolymerized onto mesoporous TiO_2 electrodes," *Inorganica Chimica Acta*, vol. 359, no. 12, pp. 3871–3874, 2006.

[22] L. F. Cueto, G. A. Hirata, and E. M. Sánchez, "Thin-film TiO_2 electrode surface characterization upon CO_2 reduction processes," *Journal of Sol-Gel Science and Technology*, vol. 37, no. 2, pp. 105–109, 2006.

[23] J. C. S. Wu and H. M. Lin, "Photo reduction of CO_2 to methanol via TiO_2 photocatalyst," *International Journal of Photoenergy*, vol. 7, no. 3, pp. 115–119, 2005.

[24] O. Ozcan, F. Yukruk, E. U. Akkaya, and D. Uner, "Dye sensitized CO_2 reduction over pure and platinized TiO_2 ," *Topics in Catalysis*, vol. 44, no. 4, pp. 523–528, 2007.

[25] T. Nakagawa, "Separation mechanism of gas separation mebrane," *Hyoumen*, vol. 26, no. 7, pp. 499–509, 1988.

[26] A. Nishimura, N. Sugiura, M. Fujita, S. Kato, and S. Kato, "Influence of preparation conditions of coated TiO_2 film on CO_2 reforming performance," *Kagaku Kogaku Ronbunshu*, vol. 33, no. 2, pp. 146–153, 2007.

[27] A. Nishimura, M. Fujita, S. Kato, and S. Kato, "CO_2-reforming performance of coated TiO_2 film with supported metal," *Kagaku Kogaku Ronbunshu*, vol. 33, no. 5, pp. 432–438, 2007.

[28] A. Nishimura, N. Sugiura, S. Kato, N. Maruyama, and S. Kato, "High yield CO_2 conversion into CH_4 by photocatalyst multilayer film," in *Proceedings of the 2nd International Energy Conversion Engineering Conference (AIAA '04)*, August 2004, AIAA 2004-5619.

[29] A. Nishimura, N. Sugiura, M. Fujita, S. Kato, and S. Kato, "Influence of photocatalyst film forming conditions on CO_2 reforming," in *Proceedings of the 3rd International Energy Conversion Engineering Conference (AIAA '05)*, August 2005, AIAA 2005-5536.